

Mesoproterozoic $^{40}\text{Ar}/^{39}\text{Ar}$ age and Sr–Nd isotopic geochemistry of calc-alkaline lamprophyre from the Mudigubba area, Eastern Dharwar Craton, India

Ashutosh Pandey¹, N. V. Chalapathi Rao^{1,*} and Ramananda Chakrabarti²

¹Department of Geology, Institute of Science, Banaras Hindu University, Varanasi 221 005, India

²Centre for Earth Sciences, Indian Institute of Science, Bengaluru 560 012, India

We report a $^{40}\text{Ar}/^{39}\text{Ar}$ Mesoproterozoic radiometric age for a calc-alkaline lamprophyre dyke from the Mudigubba area towards the western margin of the Cuddapah Basin, Eastern Dharwar Craton (EDC), Southern India. Amphibole phenocryst separates from this lamprophyre yielded a plateau age of 1169 ± 8 Ma (2σ), which is almost 50 million years older than the majority of radiometric dates available for the Wajrakarur field kimberlites which are proximal to this dyke. Bulk-rock Sr–Nd isotopic analyses of the Mudigubba lamprophyre dykes ($\epsilon\text{Nd}_{(t)}$ between -13.3 and -12.4) reveal their derivation from an old, enriched, continental lithospheric mantle unlike the kimberlites (bulk-rock and perovskite *in situ* $\epsilon\text{Nd}_{(t)}$ between -0.77 and $+7.93$), which originated either from a chondritic or depleted mantle source. This study provides further evidence for emplacement of compositionally distinct, mantle-derived Mesoproterozoic alkaline magmas in the EDC and highlights the extremely heterogeneous character of the lithospheric mantle beneath this craton.

Keywords: Alkaline magma, lamprophyre dyke, lithospheric mantle, kimberlites, radiometric age.

THE Eastern Dharwar Craton (EDC) in the southern Indian shield hosts numerous Precambrian deep, mantle-derived alkaline rocks such as kimberlites, lamprophyres, lamproites and carbonatites^{1–4}. Majority of these widespread kimberlites are known to be ~ 1.1 Gyr old⁵ and are considered to have been derived from a sub-continental lithospheric mantle^{1,6,7}. However, a sub-lithospheric mantle derivation of these kimberlites has also been suggested^{8,9}. The Wajrakarur kimberlite field (WKF) of the EDC also hosts shoshonitic lamprophyre dykes at Udiripikonda, Sivarampetta and Korakkodu, which are inferred to be derived from a relatively shallower lithospheric mantle compared to the coeval diamondiferous kimberlites^{10–13}.

*For correspondence. (e-mail: nvrao@bhu.ac.in)

Recently, calc-alkaline lamprophyres tapping a subduction-metasomatized sub-continental lithospheric mantle source and located closer to the western margin of the Cuddapah Basin in the EDC have been described from two localities – (i) the Mudigubba area (to the east of Ramagiri–Penakcherla schist belt) and (ii) in the Kadiri schist belt (Figure 1)^{14,15}. However, the age of these lamprophyres remains unknown. The present study examines the temporal and genetic relationship, if any, between the ~ 1.1 Gyr Mesoproterozoic kimberlites and related magmatism (ultramafic lamprophyres and carbonatites), and the calc-alkaline lamprophyres in the EDC using $^{40}\text{Ar}/^{39}\text{Ar}$ radiometric dating of amphibole separates and whole-rock Sr–Nd isotopic analyses of the Mudigubba calc-alkaline lamprophyre dykes.

Sampling and analytical protocol

Fresh samples from the lamprophyre dykes exposed to the NNW of Mudigubba (MUD, Figure 1) ($14^{\circ}23'34.9''\text{N}$; $77^{\circ}58'43.3''\text{E}$) in the EDC were collected and the rock chips were powdered for whole-rock Sr–Nd isotope analyses. These dykes intrude the hornblende biotite gneissic rocks and strike in NE–SW direction. The presence of large amphibole phenocrysts set in a felsic groundmass giving rise to the typical porphyritic–panidiomorphic texture was well apparent in the hand specimens (Figure 1c and d). Petrography revealed that these rocks were characterized by the presence of amphibole phenocrysts along with amphibole and clinopyroxene microphenocrysts, whereas feldspar, apatite and titanite were essentially confined to the groundmass (Figure 1e and f)¹⁴.

Amphibole phenocrysts were separated from one of the lamprophyre samples for $^{40}\text{Ar}/^{39}\text{Ar}$ analysis by incremental heating technique. Mineral separates weighing about 0.02 g were cleaned in an ultrasonic bath using deionized water and subsequently packed in aluminium capsules. Samples of the Minnesota hornblende (MMhb-1, age 523.1 ± 2.6 Ma) along with high-purity CaF_2 and K_2SO_4 salts constituted the monitor samples¹⁶. High-purity nickel

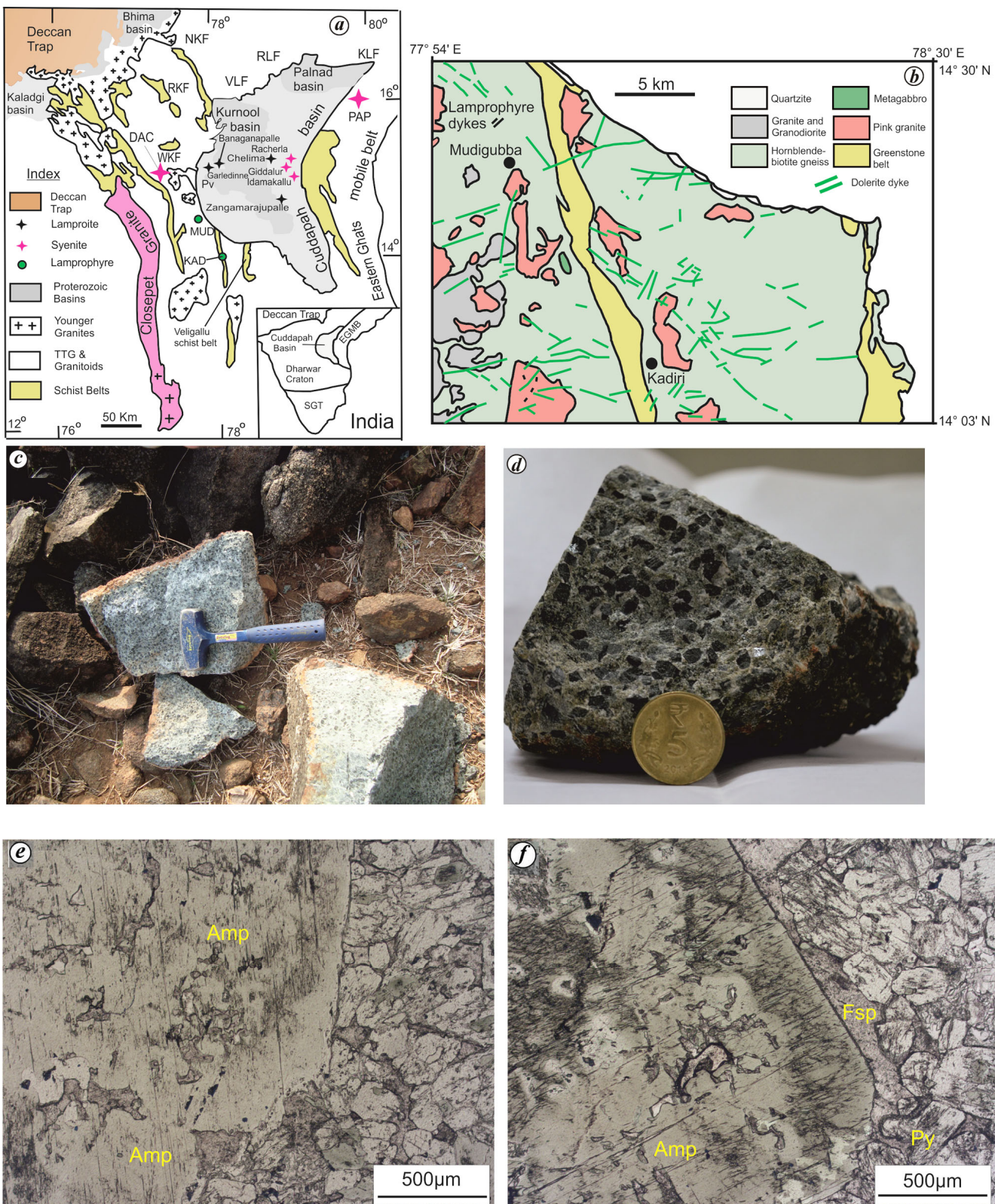


Figure 1. *a*, Geological map of the Eastern Dharwar Craton (EDC), India (after Naqvi²⁵) showing locations of the kimberlite fields – RKF (Rairur kimberlite field), NKF (Narayanpet kimberlite field) and WKF (Wajrakarur kimberlite field); lamproite fields – KLF (Krishna lamproite field), RLF (Ramadugu lamproite field) and VLF (Vattikod lamproite field), and calc-alkaline lamprophyres at Mudigubba (MUD) and Kadiri schist belt (KAD). PAP, Prakasam Alkaline Province and DAC, Dancherla Alkaline Complex. *b*, Geological map of the study area (modified after Pandey *et al.*¹⁴) showing locations and trend of Mudigubba calc-alkaline lamprophyre dykes. (*c*, *d*) Hand specimens and (*e*, *f*) photomicrographs of lamprophyre dyke samples. Amp, Amphibole; Fsp, Feldspar and Py, Pyroxene.

Table 1. $^{40}\text{Ar}/^{39}\text{Ar}$ age data for amphibole phenocrysts of the Mudigubba calc-alkaline lamprophyre (sample PP/MUD6/2) ($J = 0.000474962 \pm 0.0000024$)

Temperature (°C)	$^{36}\text{Ar}/^{39}\text{Ar}$ ($\pm 2\sigma$)	$^{40}\text{Ar}/^{39}\text{Ar}$ ($\pm 2\sigma$)	Apparent age (Myr) ($\pm 2\sigma$)	$^{39}\text{Ar}\%$	$^{40}\text{Ar}^*\%$	$^{37}\text{Ar}/^{39}\text{Ar}$ ($\pm 2\sigma$)	$^{40}\text{Ar}/^{36}\text{Ar}$ ($\pm 2\sigma$)
400	0.66565 ± 0.0147	211.799 ± 4.591	34.9 ± 31.3	1.16	15.47	21.3484 ± 8.3723	349.6 ± 25.2
450	0.23656 ± 0.00497	118.25 ± 2.021	71.1 ± 6.18	2.56	56.43	22.218 ± 3.2281	678.3 ± 49
700	0.05503 ± 0.00316	1098.7 ± 22.275	837.4 ± 47	2.15	99.48	12.7346 ± 6.153	56745.3 ± 52426.4
750	0.05756 ± 0.0037	1307.51 ± 37.204	969.5 ± 47.5	1.88	99.57	13.763 ± 5.1341	68743.2 ± 57959.9
800	0.08785 ± 0.00283	982.63 ± 31.663	798.6 ± 40.7	3.86	98.87	17.9986 ± 4.6371	26240.6 ± 10019.1
850	0.06629 ± 0.0017	995.395 ± 15.418	827.5 ± 32.3	4.13	99.69	19.9807 ± 3.9086	96350.7 ± 104428.5
900	0.48068 ± 0.00276	2045.61 ± 40.554	1172.8 ± 18.8	3.17	93.11	1.2927 ± 0.4346	4287.9 ± 195.8
950	0.16839 ± 0.00237	1773.09 ± 36.303	1166.6 ± 18.4	4.67	97.66	10.0249 ± 0.381	12636.5 ± 635.1
1000	0.2996 ± 0.00161	1984.19 ± 28.242	1176.5 ± 13	6.74	95.63	2.1286 ± 0.2169	6757.3 ± 171.4
1100	6.85333 ± 0.02814	3944.53 ± 19.723	1168.94 ± 9.61	31.77	48.66	0.0218 ± 0.0267	575.6 ± 9.4
1150	1.91487 ± 0.00673	2482.66 ± 12.413	1168.42 ± 5.68	12.81	77.21	0.0951 ± 0.0617	1296.7 ± 14
1200	5.30461 ± 0.10587	3468.83 ± 17.344	1161.6 ± 16.1	7.41	54.81	0.1071 ± 0.0572	654 ± 22.2
1300	0.09346 ± 0.00688	1651.44 ± 24.596	1169.1 ± 13.6	17.69	99.1	15.4918 ± 0.4199	32982 ± 5243.8
Total	2.71531 ± 0.01122	2450.13 ± 8.469	1100.93 ± 6.63	100	67.49	6.9548 ± 0.3686	908.9 ± 11.6

wires were placed in the sample and also in the monitor capsules for checking the neutron influence variation (~5%). Aluminium capsules, placed in a 0.5 mm thick Cd cylinder, were irradiated in the heavy-water-moderated DHRUVA reactor at the Bhabha Atomic Research Centre (BARC), Mumbai, for ~100 h. Following the irradiation, the samples were wrapped in aluminium foil and loaded in the extraction unit of a noble gas system (Thermo Fisher Scientific, USA). Argon extraction was carried out in a series of steps up to 1300°C in an electrically heated ultrahigh vacuum furnace. The argon released in each step, after purification by deploying Ti-Zr getters, was analysed using a mass spectrometer (Thermo Fisher ARGUS VI, USA), at the $^{40}\text{Ar}-^{39}\text{Ar}$ Laboratory in the Department of Earth Sciences, Indian Institute of Technology (IIT) Bombay, Mumbai. The mass spectrometer deployed five Faraday cups fitted with $10^{11} \Omega$ resistors.

Interference corrections for Ca- and K-derived Ar isotopes were performed from the analysis of CaF_2 and K_2SO_4 salts using $(^{36}\text{Ar}/^{37}\text{Ar})\text{Ca}$, $(^{39}\text{Ar}/^{37}\text{Ar})\text{Ca}$ and $(^{40}\text{Ar}/^{39}\text{Ar})\text{K} = 0.0028006$, 0.009528 and 0.002829 respectively. The ^{40}Ar blank contributions were <1–2% in all temperature steps. The irradiation parameter J was corrected for neutron flux variation using the activity of nickel wires irradiated along with each sample. The plateau ages reported comprise a minimum of 84.3% of the total ^{39}Ar released along with four or more successive degassing steps where the mean ages overlap at the 2σ level, which excludes the error contribution (0.5%) from the J value. Table 1 presents the results.

Rock chips of four samples were crushed and powdered followed by dissolution using a mixture of concentrated HF, HNO_3 and HCl in screw-cap Teflon vials. A multi-step ion exchange column chromatography method employing AG50W X8 resin (BioRad) was used to separate Sr and Nd. Strontium was eluted using 3N

HCl from a AG50W X8 (100–200 mesh) resin, whereas REE were eluted using 6N HCl. Neodymium separation from the rest of the REE was done using 0.2M 2-hydroxyisobutyric acid ($\text{pH} = 4.495$) from a AG50W X8 (200–400 mesh) resin. The isotope ratios were measured using a thermal ionization mass spectrometer (TIMS; Thermo Scientific Triton Plus) at the Indian Institute of Science (IISc), Bengaluru employing established protocols¹⁷. Briefly, Sr isotope ratios were measured by a single oxidized Ta filament assembly, whereas a double Re filament set was used for Nd isotope ratio measurements. To correct for instrumental mass fractionation, the measured $^{87}\text{Sr}/^{86}\text{Sr}$ and $^{143}\text{Nd}/^{144}\text{Nd}$ ratios were normalized to $^{86}\text{Sr}/^{88}\text{Sr} = 0.1194$ and $^{146}\text{Nd}/^{144}\text{Nd} = 0.7219$ respectively. During the course of the study, JNDI-1 Nd isotopic standard and SRM-987 Sr isotopic standard were analysed. Uncertainties in $^{143}\text{Nd}/^{144}\text{Nd}$ (measured) were better than 5 in the sixth decimal place and for $^{87}\text{Sr}/^{86}\text{Sr}$ ratios, they were better than 9 in the sixth decimal place. Table 2 provides the results.

Results and discussion

Table 1 shows the results of $^{40}\text{Ar}-^{39}\text{Ar}$ geochronology and Figure 2 shows the variation in apparent age with cumulative $^{39}\text{Ar}\%$. Step heating was carried out in 13 steps from 400°C to 1300°C yielding a plateau age of 1169 ± 8 Ma (2σ) with MSWD = 0.41 (Figure 2a). The apparent age of >1100 Ma corresponded to 84.3% of the total ^{39}Ar released and was observed after 18% cumulative ^{39}Ar loss. In a plot of $^{40}\text{Ar}/^{36}\text{Ar}$ versus $^{39}\text{Ar}/^{36}\text{Ar}$, an apparent age of 1177 ± 20 Ma (2σ , MSWD = 0.04) with initial $^{40}\text{Ar}/^{36}\text{Ar} = 287 \pm 19$ was obtained (Figure 2b). An age of 1171 ± 12 Ma (2σ , MSWD = 0.13) along with an initial $^{40}\text{Ar}/^{36}\text{Ar} = 287 \pm 19$ was also obtained on a $^{36}\text{Ar}/^{40}\text{Ar}$ versus $^{39}\text{Ar}/^{40}\text{Ar}$ variation diagram (Figure 2c).

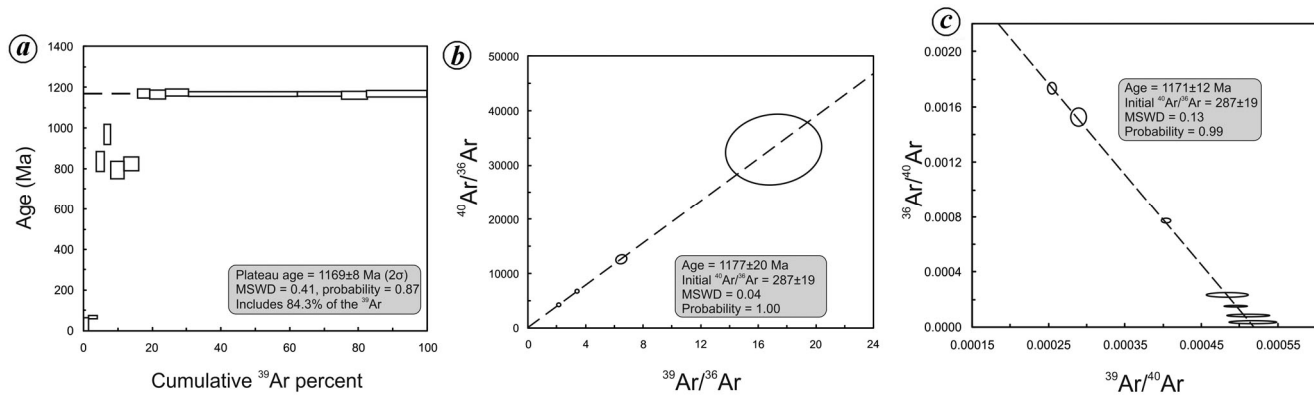


Figure 2. $^{40}\text{Ar}/^{39}\text{Ar}$ spectra and isochron diagram for amphibole separates from the Mudigubba lamprophyre dyke.

Table 2. Bulk-rock Sr–Nd isotopic abundances in the Mudigubba calc-alkaline lamprophyres (the present study) compared with those of other co-spatial calc-alkaline lamprophyres from the Eastern Dharwar craton

Rb-Sr isotopic composition

Locality	Sample	Rb (ppm)	Sr (ppm)	$^{87}\text{Sr}/^{86}\text{Sr}$	$^{87}\text{Rb}/^{86}\text{Sr}$	$^{87}\text{Sr}/^{86}\text{Sr} (t)$
Mudigubba ^a	PP/MUD7/1	17	382	0.707124	0.1288	0.704968
Mudigubba ^a	PP/MUD1/1	28	479	0.707564	0.1692	0.704732
Mudigubba ^a	PP/MUD2/1	26	354	0.708525	0.2126	0.704967
Mudigubba ^a	PP/MUD3/1	19	327	0.707146	0.1682	0.704331
Udiripikonda ^b	UK/2012/2	137	1602	0.709230	0.2476	0.705333
Udiripikonda ^b	PP/U1/1	94	1395	0.709294	0.1951	0.706223
Udiripikonda ^b	PP/U1/3	159	1447	0.710909	0.3181	0.705900
Udiripikonda ^c	UDPL-1	105	1215	0.709520	0.2493	0.705600
Korakodu ^d	PP/KD1/3	179	1537	0.713426	0.3373	0.708117
Korakodu ^d	PP/KD2/2	172	1546	0.712658	0.3222	0.707586
Sivarampet ^e	SHLM-1	93	710	0.712980	0.0510	0.712180
Sivarampet ^e	S1/2	104	854	0.731765	0.3527	0.708213
Sivarampet ^e	S1/3	81	752	0.713418	0.3119	0.708507

Sm–Nd isotopic composition

Locality	Sample	Sm (ppm)	Nd (ppm)	$^{143}\text{Nd}/^{144}\text{Nd}$	$^{147}\text{Sm}/^{144}\text{Nd}$	$^{143}\text{Nd}/^{144}\text{Nd} (t)$	$\varepsilon\text{Nd}(t)$	TDM (Gyr)
Mudigubba ^a	PP/MUD7/1	6.7	29.4	0.511553	0.1377	0.510496	-12.40	2.80
Mudigubba ^a	PP/MUD1/1	7.1	32.3	0.511494	0.1329	0.510474	-12.80	2.75
Mudigubba ^a	PP/MUD2/1	8.9	38.7	0.511529	0.1390	0.510462	-13.00	2.89
Mudigubba ^a	PP/MUD3/1	8.4	36.2	0.511523	0.1403	0.510447	-13.30	2.94
Udiripikonda ^b	UK/2012/2	12.1	78.6	0.510737	0.0930	0.510065	-22.50	2.8
Udiripikonda ^b	PP/U1/1	11.4	76.9	0.510839	0.0896	0.510192	-20.10	2.6
Udiripikonda ^b	PP/U1/3	13.0	86.4	0.510828	0.0909	0.510172	-20.50	2.6
Udiripikonda ^c	UDPL-1	8.5	58.9	0.510850	0.0873	0.510220	-19.57	-
Korakodu ^d	PP/KD1/3	11.4	84.7	0.511002	0.0813	0.510415	-15.70	2.28
Korakodu ^d	PP/KD2/2	13.3	92.2	0.510676	0.0872	0.510047	-22.90	2.74
Sivarampet ^e	SHLM-1	6.1	38.2	0.511000	0.0664	0.510520	-13.73	-
Sivarampet ^e	S1/2	8.9	50.6	0.511011	0.1063	0.510244	-19.1	2.75
Sivarampet ^e	S1/3	8.0	48.7	0.510695	0.0993	0.509978	-24.2	2.98

^aThe present study. Initial values calculated for an emplacement age of 1169 Ma. Rb, Sr, Sm and Nd data are from ICPMS analysis.

$$\varepsilon\text{Nd}(t) = \left(\frac{^{143}\text{Nd}}{^{144}\text{Nd}}_{\text{sample}(t)} - \frac{^{143}\text{Nd}}{^{144}\text{Nd}}_{\text{CHUR}(t)} - 1 \right) \times 10^4.$$

$$T_{\text{DM}} = (1/\lambda) \times \ln(1 + \frac{^{143}\text{Nd}}{^{144}\text{Nd}}_{\text{sample}} - \frac{^{143}\text{Nd}}{^{144}\text{Nd}}_{\text{DM}} / \frac{^{147}\text{Sm}}{^{144}\text{Nd}}_{\text{sample}} - \frac{^{147}\text{Sm}}{^{144}\text{Nd}}_{\text{DM}}).$$

Present-day CHUR values²⁶, $^{147}\text{Sm}/^{144}\text{Nd} = 0.1967$ and $^{143}\text{Nd}/^{144}\text{Nd} = 0.512638$.

Data sources: ^bPandey *et al.*¹⁰, ^cKhan *et al.*¹¹, ^dRaguvanshi *et al.*¹², ^ePankaj *et al.*¹³.

Precise dating of kimberlites is a challenging task¹⁸ and it is evident from a large range in radiometric ages published for the Mesoproterozoic kimberlites of the EDC with a few dates showing very high error range (Chalap-

thi Rao *et al.*¹ and references therein). Majority of the kimberlite pipes of the EDC are dated to be <1100 Myr (refs 1, 5). It is evident that the Mudigubba calc-alkaline lamprophyre analysed in this study was emplaced during

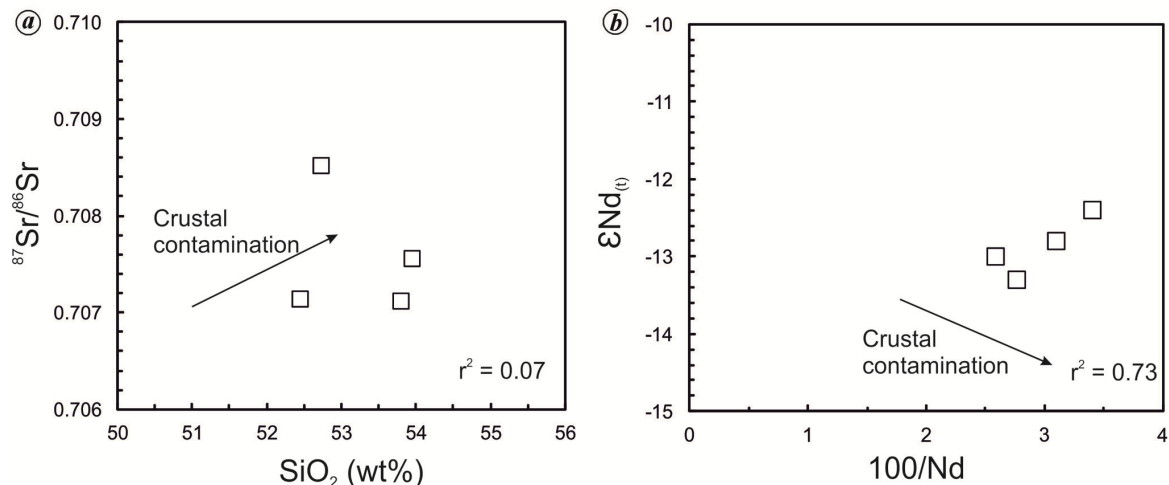


Figure 3. (a) SiO_2 (wt%) versus ${}^{87}\text{Sr}/{}^{86}\text{Sr}$ and (b) $100/\text{Nd}$ versus $\varepsilon\text{Nd}_{(\text{t})}$ variation diagram for the Mudigubba calc-alkaline lamprophyres.

the Mesoproterozoic, but approximately 50 Myr earlier than the time of peak kimberlite magmatism in the EDC. The age of this lamprophyre dyke also post-dates that of the Mesoproterozoic lamproites (1225 to 1400 Myr; Krishna, Ramadugu, Vattikod, and Chelima lamproites) in the EDC^{19–21}. Further detailed studies are required to date more precisely the ages of various lamprophyres in this domain in future, to constrain the timing of lamprophyre emplacement.

The ${}^{87}\text{Sr}/{}^{86}\text{Sr}$ and ${}^{143}\text{Nd}/{}^{144}\text{Nd}$ measured isotopic values in the studied lamprophyres ranged between 0.707124 and 0.708525 as well as 0.511494 and 0.511553 respectively (Table 2). ${}^{87}\text{Sr}/{}^{86}\text{Sr}$ initial ratios, obtained assuming an emplacement age of 1169 Myr, ranged between 0.704331 and 0.704968, whereas ${}^{143}\text{Nd}/{}^{144}\text{Nd}$ initial ratios ranged between 0.510447 and 0.511553, which translates to $\varepsilon\text{Nd}_{(\text{t})} = -12.4$ to -13.3 (Table 2). Based on whole-rock trace elements geochemistry, Pandey *et al.*¹⁴ inferred that these dykes were derived from the sub-lithospheric mantle previously metasomatized by fluid-related subduction event probably during the Neoarchean. The ${}^{87}\text{Sr}/{}^{86}\text{Sr}$ of these dykes were poorly correlated ($r^2 = 0.07$) with increasing silica content, which is an index of granitic crustal assimilation, ruling out any role of crustal contamination (Figure 3 a). This was further corroborated by a good correlation between $\varepsilon\text{Nd}_{(\text{t})}$ and $100/\text{Nd}$ ($r^2 = 0.73$), as crustal contamination imparts most unradiogenic Nd isotopic character to the samples with the lowest Nd concentrations²² (Figure 3 b). These correlations suggest that the Mudigubba calc-alkaline lamprophyre dykes suffered negligible crustal contamination and their geochemistry reflects the composition of the mantle source from which they are derived. Strongly negative $\varepsilon\text{Nd}_{(\text{t})}$ values along with a Neoarchean Nd depleted mantle model age (T_{DM} , 2.75–2.94 Gyr) suggest that the primary magma were derived from an ancient metasomatized sub-continental lithospheric mantle source.

The calc-alkaline as well as the shoshonitic lamprophyres of the EDC have distinct Sr–Nd isotopic composition compared to those of the kimberlites (Figure 4). The kimberlites (with $\varepsilon\text{Nd}_{(\text{t})} > 0$) are derived from a significantly more depleted mantle source compared to the coeval lamproites (with $\varepsilon\text{Nd}_{(\text{t})}$ ranging between -4.44 and -2.66) in the Bastar Craton²³ and Mesoproterozoic (~1.2–1.4 Ga) lamproites (Krishna, Ramadugu, Vattikod and Chelima) of the EDC^{19–21}. The lamprophyres, on the other hand, have extremely radiogenic ${}^{87}\text{Sr}/{}^{86}\text{Sr}_{(\text{t})}$ (0.704331–0.712180) and strongly negative $\varepsilon\text{Nd}_{(\text{t})}$ (-22.9 to -12.4), suggesting derivation from an enriched sub-continental lithospheric mantle source. It should be noted that there was a large variation in the ${}^{87}\text{Sr}/{}^{86}\text{Sr}$ ratio in the kimberlites with almost constant Nd isotopic values akin to those exhibited by the coeval Sakri lamproites from the Nuapada field in the Bastar Craton (Figure 4). Such a variation is ascribed to the presence of phlogopite in the mantle source region²⁴. Similar variations were observed in the Kadiri lamprophyres and from elevated Rb/Sr ratio in these dykes, which show similarity with those from the phlogopite lherzolite xenoliths found in the kimberlites of the Kaapval Craton¹⁵. The Mudigubba calc-alkaline lamprophyres, on the other hand, exhibited restricted initial Sr–Nd isotopic variation (Figure 4), inconsistent with the presence of metasomatic phlogopite in the source. This is in accordance with variable Ba/Rb and low Rb/Sr ratios in these dykes revealing the presence of amphibole in the source¹⁴. These results demonstrate that the spatially widespread Mesoproterozoic mantle-derived alkaline magmatism in the southern Indian shield displays extensive compositional diversity.

Conclusion

${}^{40}\text{Ar}/{}^{39}\text{Ar}$ dating of amphibole phenocryst separates from a calc-alkaline lamprophyre occurring near Mudigubba

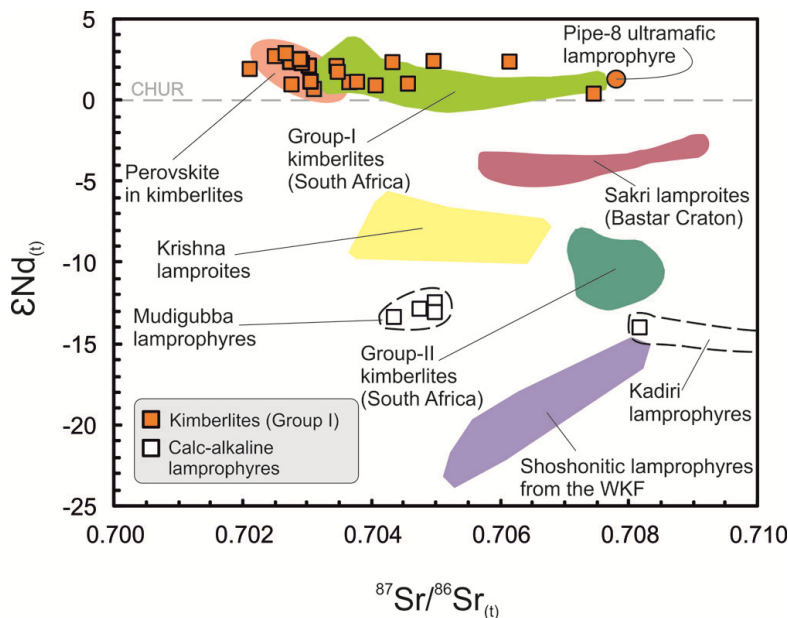


Figure 4. Plot of $^{87}\text{Sr}/^{86}\text{Sr}(t)$ versus $\varepsilon\text{Nd}_{(t)}$ for the Mesoproterozoic kimberlites, shoshonitic and calc-alkaline lamprophyres from the EDC. Compositional fields for the archetypical groups I and II kimberlites from South Africa are from Becker and Le Roex²⁷, and isotopic data of perovskite as well as bulk-rock group I ~1100 Myr kimberlites from the EDC are from Chalapathi Rao *et al.*^{1,28}, Paton *et al.*^{8,9} and Sharma *et al.*²⁹. Data of ~1045 Ma Sakri lamproites, Nuapada lamproite field of the Bastar Craton²³ and 1.2 Ga Krishna lamproites from the EDC²⁰ are also shown for comparison. Composition of pipe-8 intrusion in the WKF, which is now reclassified as an ultramafic lamprophyre is from Dongre *et al.*³⁰. Data sources for the shoshonitic lamprophyres from WKF are given in Table 2. CHUR, Chondritic Uniform Reservoir.

gave a plateau age of 1169 ± 8 Ma. The obtained age suggests that few calc-alkaline lamprophyres in the EDC were emplaced about 50 Myr earlier than the peak kimberlite magmatism during the Mesoproterozoic. Sr-Nd isotopic ratios of the shoshonitic and calc-alkaline lamprophyres from the WKF were strikingly different from those of the kimberlites, revealing that the former tapped a continental lithospheric mantle source. The later erupted kimberlites, in contrast, were derived either from a deep sub-lithospheric source or from the base of the sub-continental lithospheric mantle enriched by melts derived from the asthenosphere. This study suggests that the cratonic lithospheric mantle beneath the EDC was extremely heterogeneous and generated geochemically diverse alkaline magma during the Mesoproterozoic.

- Chalapathi Rao, N. V., Wu, F.-Y., Mitchell, R.H., Li, Q.-L. and Lehmann, B., Mesoproterozoic U-Pb ages, trace element and Sr-Nd isotopic composition of perovskite from kimberlites of the Eastern Dharwar Craton, southern India: distinct mantle sources and a widespread 1.1 Ga tectonomagmatic event. *Chem. Geol.*, 2013, **353**, 48–64.
- Chalapathi Rao, N. V., Giri, R. K., Sharma, A. and Pandey, A., Lamprophyres from the Indian shield: a review of their occurrence, petrology, tectonomagmatic significance and relationship with the Kimberlites and related rocks. *Episodes*, 2020, **43**(1), 231–248.
- Smith, C. B., Haggerty, S. E., Chatterjee, B., Beard, A. and Townsend, R., Kimberlite, lamproite, ultramafic lamprophyre, and carbonatite relationships on the Dharwar Craton, India; an exam-

ple from the Khaderpet pipe, a diamondiferous ultramafic with associated carbonatite intrusion. *Lithos*, 2013, **182–183**, 102–113.

- Devaraju, T. C., Laajoki, K., Zozulya, D., Khanadali, S. D. and Ugarkar, A. G., Neo-proterozoic dyke swarms of southern Karnataka: Part II: geochemistry, oxygen isotope composition, Rb-Sr age and petrogenesis. *Mem. Geol. Soc. India*, 1995, **33**, 267–306.
- Pandey, A. and Chalapathi Rao, N. V., Supercontinent transition as a trigger for ~1.1 Gyr diamondiferous kimberlites and related magmatism in India. *Lithos*, 2020, **370–371**, 105620.
- Kumar, A., Heaman, L. M. and Manikyamba, C., Mesoproterozoic kimberlites in south India: a possible link to ~1.1 Ga global magmatism. *Precambrian Res.*, 2007, **154**, 192–204.
- Chalapathi Rao, N. V., Creaser, R. A., Lehmann, B. and Panwar, B. K., Re-Os isotopic study of Indian kimberlites and lamproites: implications for mantle source regions and cratonic evolution. *Chem. Geol.*, 2013, **353**, 36–47.
- Paton, C., Hergt, J. M., Phillips, D., Woodhead, J. D. and Shee, S. R., New insights into the genesis of Indian kimberlites from the Dharwar Craton via *in situ* Sr isotope analysis of groundmass perovskite. *Geology*, 2007, **35**, 1011–1014.
- Paton, C., Hergt, J. M., Phillips, D. and Shee, S. R., Identifying the asthenospheric component of kimberlite magmas from the Dharwar Craton, India. *Lithos*, 2009, **112S**, 296–310.
- Pandey, A., Chalapathi Rao, N. V., Chakrabarti, R., Pandit, D., Pankaj, P., Kumar, A. and Sahoo, S., Petrogenesis of a Mesoproterozoic shoshonitic lamprophyre dyke from the Wajrakarur kimberlite field, eastern Dharwar Craton, southern India: geochemical and Sr-Nd isotopic evidence for a modified sub-continental lithospheric mantle source. *Lithos*, 2017, **292–293**, 218–233.
- Khan, S., Dongre, A., Viljoen, F., Li, Q.-L. and Le Roux, P., Petrogenesis of lamprophyres synchronous to kimberlites from the Wajrakarur kimberlite field: implications for contrasting lithospheric mantle sources and geodynamic evolution of the eastern

- Dharwar Craton of southern India. *Geol. J.*, 2019, **54**(5), 2994–3016.
12. Raghuvanshi, S., Pandey, A., Pankaj, P., Chalapathi Rao, N. V., Chakrabarti, R., Pandit, D. and Pandey, R., Lithosphere–asthenosphere interaction and carbonatite metasomatism in the genesis of Mesoproterozoic shoshonitic lamprophyres at Korakkodu, Wajrakarur kimberlite field, Eastern Dharwar Craton, southern India. *Geol. J.*, 2019, **54**(5), 3060–3077.
 13. Pankaj, P., Giri, R. K., Chalapathi Rao, N. V., Chakrabarti, R. and Raghuvanshi, S., Mineralogy and petrology of shoshonitic lamprophyre dykes from the Sivarampetta area, diamondiferous Wajrakarur Kimberlite Field, Eastern Dharwar Craton, southern India. *J. Mineral. Petrol. Sci.*, 2020, <https://doi.org/10.2465/jmps.191004b>.
 14. Pandey, A., Chalapathi Rao, N. V., Pandit, D., Pankaj, P., Pandey, R., Sahoo, S. and Kumar, A., Subduction-tectonics in the evolution of the eastern Dharwar Craton, southern India: insights from the post-collisional calc-alkaline lamprophyres at the western margin of the Cuddapah Basin. *Precambrian Res.*, 2017, **298**, 235–251.
 15. Pandey, A., Chalapathi Rao, N. V., Chakrabarti, R., Pankaj, P., Pandit, D., Pandey, R. and Sahoo, S., Post-collisional calc-alkaline lamprophyres from the Kadiri greenstone belt: evidence for the Neoarchean convergence-related evolution of the Eastern Dharwar Craton and its schist belts. *Lithos*, 2018, **320–321**, 105–117.
 16. Renne, P. R., Swisher, C. C., Deino, A. L., Karner, D. B., Owens, T. L. and DePaolo, D. J., Intercalibration of standards, absolute ages and uncertainties in $^{40}\text{Ar}/^{39}\text{Ar}$ dating. *Chem. Geol.*, 1998, **145**, 117–152.
 17. Banerjee, A., Chakrabarti, R. and Mandal, S., Geochemical anatomy of a spheroidally weathered diabase. *Chem. Geol.*, 2016, **440**, 124–138.
 18. Heaman, L. M., Phillips, D. and Pearson, G., Dating kimberlites: methods and emplacement patterns through time. *Elements*, 2019, **15**(6), 399–404.
 19. Chalapathi Rao, N. V., Gibson, S. A., Pyle, D. M. and Dickin, A. P., Contrasting isotopic mantle sources for Proterozoic lamproites and kimberlites from the Cuddapah Basin and Eastern Dharwar Craton: implication for Proterozoic mantle heterogeneity beneath southern India. *J. Geol. Soc. India*, 1998, **52**(6), 683–694.
 20. Chakrabarti, R., Basu, A. R. and Paul, D. K., Nd–Hf–Sr–Pb isotopes and trace element geochemistry of Proterozoic lamproites from southern India: subducted komatiite in the source. *Chem. Geol.*, 2007, **236**, 291–302.
 21. Talukdar, D., Pandey, A., Chalapathi Rao, N. V., Kumar, A., Pandit, D., Belyatsky, B. and Lehmann, B., Petrology and geochemistry of the Mesoproterozoic Vattikod lampreites, Eastern Dharwar Craton, southern India: evidence for multiple enrichment of sub-continental lithospheric mantle and links with amalgamation and break-up of the Columbia supercontinent. *Contrib. Mineral. Petrol.*, 2018, **173**, 67.
 22. McCulloch, M. T., Jaques, A. L., Nelson, D. R. and Lewis, J. D., Nd and Sr isotopes in kimberlites and lamproites from Western Australia: an enriched mantle origin. *Nature*, 1983, **302**, 400–403.
 23. Chalapathi Rao, N. V. et al., Petrology, $^{40}\text{Ar}/^{39}\text{Ar}$ age, Sr–Nd isotope systematic, and geodynamic significance of an ultrapotassic (lamproitic) dyke with affinities to kamacite from the easternmost margin of the Bastar Craton, India. *Mineral. Petrol.*, 2016, **110**, 269–293.
 24. Tappe, S., Romer, R. L., Stracke, A., Steenfelt, A., Smart, K. A., Muehlenbachs, K. and Torsvik, T. H., Sources and mobility of carbonate melts beneath cratons, with implications for deep carbon cycling, metasomatism and rift initiation. *Earth Planet. Sci. Lett.*, 2017, **466**, 152–167.
 25. Naqvi, S. M., *Geology and Evolution of the Indian Plate (from Hadean to Holocene – 4 Ga to 4 Ka)*, Capital Publishing Company, New Delhi, 2005, p. 450.
 26. Jacobsen, S. B. and Wasserburg, G. J., Sm–Nd isotopic evolution of chondrites. *Earth Planet. Sci. Lett.*, 1980, **50**, 139–155.
 27. Becker, M. and Le Roex, A. P., Geochemistry of South African on- and off-craton, group I and II kimberlites: petrogenesis and source region evolution. *J. Petrol.*, 2006, **47**(4), 673–703.
 28. Chalapathi Rao, N. V., Gibson, S. A., Pyle, D. M. and Dickin, A. P., Petrogenesis of Proterozoic kimberlites and lamproites from the Cuddapah basin and the Dharwar craton, southern India. *J. Petrol.*, 2004, **45**, 907–948.
 29. Sharma, A., Kumar, A., Pankaj, P., Pandit, D., Chakrabarti, R. and Chalapathi Rao, N. V., Petrology and Sr–Nd isotope systematics of the Ahobil kimberlite (pipe-16) from the Wajrakarur field, Eastern Dharwar Craton, southern India. *Geosci. Front.*, 2019, **10**(3), 1167–1186.
 30. Dongre, A., Viljoen, K. S., Belyanin, G., Le Roux, P. and Malandkar, M., Petrogenesis of the diamondiferous pipe-8 ultramafic intrusion from the Wajrakarur kimberlite field of southern India and its relation to the worldwide Mesoproterozoic (~1.1 Ga) magmatism of kimberlite and related rocks. *Geosci. Front.*, 2019; <https://doi.org/10.1016/j.gsf.2019.07.010>.

ACKNOWLEDGEMENTS. We thank the Head, Department of Geology, BHU, Varanasi for providing the necessary facilities. Funding for this study was provided by the DST-SERB, New Delhi, in the form of a major research project (IR/S4/ESF-18/2011) to N.V.C.R. A.P. acknowledges CSIR, New Delhi for the Shyama Prasad Mukherjee Fellowship (SPM-09/013(0262)/2018-EMR-I). We also thank Prof. Kanchan Pande (IIT Bombay) for providing the Ar–Ar geochronological data and Dr Anupam Banerjee for his help with isotopic analyses at IISc, Bengaluru. Constructive comments by an anonymous reviewer are appreciated.

Received 6 June 2020; revised accepted 23 July 2020

doi: 10.18520/cs/v119/i7/1142-1148